PERGAMON

Vision Research 41 (2001) 1437–1457

Vision Research

www.elsevier.com/locate/visres

Putting spatial attention on the map: timing and localization of stimulus selection processes in striate and extrastriate visual areas

Antígona Martínez [a], Francesco DiRusso [b], Lourdes Anllo-Vento [b], Martin I. Sereno [c], Richard B. Buxton [a], Steven A. Hillyard [b,*]

[a] *Department of Radiology, University of California, San Diego, La Jolla, CA 92093-8756, USA*
[b] *Department of Neurosciences, University of California, San Diego, La Jolla, CA 92093-0608, USA*
[c] *Department of Cognitive Science, University of California, San Diego, La Jolla, CA 92093-0109, USA*

Received 16 May 2000; received in revised form 16 August 2000

Abstract

This study investigated the cortical mechanisms of visual-spatial attention in a task where subjects discriminated patterned targets in one visual field at a time. Functional magnetic imaging (fMRI) was used to localize attention-related changes in neural activity within specific retinotopic visual areas, while recordings of event-related brain potentials (ERPs) traced the time course of these changes. The earliest ERP components enhanced by attention occurred in the time range 70–130 ms post-stimulus onset, and their neural generators were estimated to lie in the dorsal and ventral extrastriate visual cortex. The anatomical areas activated by attention corresponded closely to those showing increased neural activity during passive visual stimulation. Enhanced neural activity was also observed in the primary visual cortex (area V1) with fMRI, but ERP recordings indicated that the initial sensory response at 50–90 ms that was localized to V1 was not modulated by attention. Modeling of ERP sources over an extended time range showed that attended stimuli elicited a long-latency (160–260 ms) negativity that was attributed to the dipolar source in area V1. This finding is in line with hypotheses that V1 activity may be modulated by delayed, reentrant feedback from higher visual areas.

Keywords: Visual attention; fMRI; ERPs; Electrophysiology; Retinotopic maps

1. Introduction

It is well known that human observers can focus attention selectively within a restricted zone of the visual field and thereby facilitate the perception of stimuli at that location. Behavioral studies have shown that covertly directing attention to a specific location results in faster and more accurate detections and discriminations of stimuli within that region relative to stimuli presented outside the 'spotlight' of spatial attention (reviewed in LaBerge (1995), Wright (1998)). A good deal of behavioral and neurophysiological evidence supports the view that visual information arising from attended locations is enhanced or 'amplified' at an early stage of processing in the visual pathways, thereby improving the signal-to-noise ratio of attended inputs (Luck et al., 1994; Posner & Dehaene, 1994; Hillyard, Vogel, & Luck, 1998; Theeuwes, Kramer, & Atchley, 1999; Maunsell & McAdams, 2000).

The brain systems that control the attentional spotlight have been described as an interconnected network of cortical and subcortical structures which include the prefrontal and posterior parietal lobes, the anterior cingulate gyrus, and the pulvinar and reticular nuclei of the thalamus (Mesulam, 1990; Nobre et al., 1997; Corbetta, 1998; Hopfinger, Buonocore, & Mangun, 2000). A key unresolved question, however, concerns where and how in the visual processing pathway incoming sensory information is first modulated (i.e. either enhanced or suppressed) by spatial attention. The present study investigated this question in human subjects by combining functional magnetic resonance imag-

* Corresponding author. Tel.: +1-858-5342385; fax: +1-858-5345562.
E-mail addresses: antigona@ucsd.edu (A. Martínez), fdr@sdepl.ucsd.edu (F. DiRusso), lanllo@ucsd.edu (L. Anllo-Vento), sereno@cogsci.ucsd.edu (M.I. Sereno), rbuxton@ucsd.edu (R.B. Buxton), shillyard@ucsd.edu (S.A. Hillyard).

0042-6989/01/$ - see front matter
PII: S0042-6989(00)00267-4

ing (fMRI) with recordings of event-related brain potentials (ERPs) to define the spatio-temporal pattern of neural activity in the visual-cortical pathways as subjects performed a spatial attention task. These findings are interpreted in light of evidence from recent neurophysiological studies in animals and ERP and neuroimaging studies in humans.

1.1. Neurophysiological studies in animals

Studies in non-human primates have yielded an increasingly detailed picture of the specific visual cortical areas in which afferent information can be modulated by spatial attention. Neurophysiological recordings from monkeys have demonstrated strong influences of attention on neural activity in multiple extrastriate areas including retinotopic areas V2, V3A, and V4 as well as regions of the ventral (TEO, TE) and dorsal (MT, MST, posterior parietal lobe) processing streams (reviewed in Colby (1991), Desimone & Duncan (1995), Desimone (1998)). The general finding has been that stimuli at attended locations elicit stronger discharge in visual neurons responsive to those stimuli than do the same stimuli when attention is directed away from their location. In many situations, spatial attention appears to increase the effective strength of a stimulus as if its contrast had been increased by a multiplicative scaling or gain-control mechanism (Treue & Maunsell, 1996; Maunsell & McAdams, 2000). Particularly strong attentional modulations may be observed when attention is shifted between competing stimuli within a neuron's receptive field (Luck, Chelazzi, Hillyard, & Desimone, 1997; Reynolds, Chelazzi, & Desimone, 1999).

Recent studies in monkeys have verified the earlier report of Motter (1993) that neural activity in primary visual cortex (area V1) may also be affected by selective attention under certain conditions (Roelfsema, Lamme, & Spekreijse, 1998; Vidyasagar, 1998; Ito & Gilbert, 1999; McAdams & Maunsell, 1999). The most robust effects have been observed during discrimination tasks in which multiple, competing stimuli were present in the visual field. In some of these studies it was noteworthy that the attentional modulation began at fairly long latencies (80–100 ms or longer), considerably later than the initial sensory evoked response in V1 (Roelfsema et al., 1998; Vidyasagar, 1998). While some of this delay may be ascribed to the time required for the animal to decode the cue designating the attended stimulus, these findings raise the possibility that attentional modulations of V1 neurons may be driven by delayed feedback from higher visual-cortical areas (Vidyasagar, 1999).

This feedback hypothesis receives strong support from experiments where event-related potentials (ERPs) were recorded intracortically from multiple visual areas in monkeys who alternated attention between visual and auditory stimuli (Mehta, Ulbert, & Schroeder, 2000a; Mehta, Ulbert, & Schroeder, 2000b). Attentional modulations of the visual ERP were larger and shorter in latency at the higher ventral stream area V4 than at lower areas V2 and V1. Both the timing and laminar distribution of these attention effects supported a feedback mechanism whereby attentional amplification first occurring in higher areas was projected back to the lower areas, perhaps reducing neural refractoriness and enhancing the perceptual salience of attended stimuli. Vidyasagar (1999) has proposed further that magnocellular/dorsal stream pathways with their rapid transmission and spatial coding properties may provide feedback to earlier stages of the visual cortical pathways (including V1) to selectively facilitate inputs at attended locations before they are processed further in the ventral stream.

Neural activity in primary visual cortex can also be modulated by contextual influences from stimulus contours outside the classical receptive field. It has been suggested that the enhanced firing of V1 cells produced by such contours may reflect the grouping together of figural elements and segregation of figure from ground (Hupe et al., 1998; Ito & Gilbert, 1999; Lamme & Spekreijse, 2000). Such contextual effects may be mediated both by long-range horizontal connections within V1 and by feedback projections to V1 from higher-tier visual areas. It has been proposed that spatial attention may exert a top-down feedback influence on this V1 circuitry for figure-ground enhancement such that attended figures or objects become more perceptually salient (Roelfsema et al., 1998; Ito & Gilbert, 1999; Lamme & Spekreijse, 2000).

1.2. Studies of ERPs in humans

Electrophysiological studies in humans have found that spatial attention produces substantial modulations of evoked neural activity localized to extrastriate visual cortical areas. Stimuli presented to attended locations elicit larger P1 (latency 80–130 ms) and N1 (150–200 ms) components of the scalp-recorded visual ERP over the posterior scalp than do stimuli presented outside the spotlight of spatial attention (for reviews see Mangun (1995), Hillyard & Anllo-Vento (1998)). This amplitude enhancement of the P1 and N1 waves occurs with little or no change of the component latencies or scalp distributions, suggesting that spatial attention exerts a gain control or selective amplification of attended inputs within the visual-cortical pathways in the interval between 80–200 ms after stimulus onset (Wijers, Lange, Mulder, & Mulder, 1997; Hillyard et al., 1998). Such a gain control mechanism is consistent with proposals that paying attention to stimulus location produces a multiplicative enhancement of evoked discharge in neurons responding to the stimulus (McAdams & Maunsell, 1999).

The neural generators of the P1 and N1 components enhanced by spatial attention have been localized using techniques of scalp current density mapping, dipole modeling, and coregistration with blood-flow neuroimaging. In studies where stimuli were presented to the upper visual fields, the increased P1 positivity to attended-location stimuli could be accounted for by dipolar sources in ventral-lateral extrastriate cortex (Gomez, Clark, Luck, Fan, & Hillyard, 1994; Heinze et al., 1994b; Clark & Hillyard, 1996). In contrast, for lower-field stimuli the source of the P1 attention effect was calculated to lie in dorsal extrastriate cortex corresponding to Brodmann's areas 18/19 (Woldorff et al., 1997), suggesting that the enhanced P1 positivity was generated in retinotopically organized visual cortex. These source localizations were supported by studies that combined PET neuroimaging with ERP recordings. The calculated dipolar sources of the P1 attention effect were found to correspond closely with regions of increased cerebral blood flow in ventral (Heinze et al., 1994b) and dorsal (Woldorff et al., 1997) extrastriate occipital cortex. The enhanced N1 activity at 160–200 ms was estimated to arise from multiple generators that included sources in ventral-lateral and more anterior extrastriate areas (Gomez et al., 1994; Clark & Hillyard, 1996).

In all of the aforementioned ERP experiments, the initial C1 component (sometimes called NP80) that onsets at around 50–60 ms post-stimulus remained unaffected by spatial attention (see also Wijers et al., 1997; Lange, Wijers, Mulder, & Mulder, 1998). The C1 has a voltage topography over the occipital scalp and retinotopic properties that are consistent with a neural generator in primary visual cortex (Clark, Fan, & Hillyard, 1995). In addition, when the dipolar source calculated for the C1 was projected onto co-registered MRI sections, it was found to lie in or adjacent to the calcarine fissure that contains the primary cortex (Clark & Hillyard, 1996; Martinez et al., 1999). Thus, these ERP and PET studies, together with optical imaging evidence (Gratton, 1997), suggest that the initial afferent response evoked in striate cortex is not affected by spatial attention and that the earliest attentional modulation of visual information flow instead takes place in higher, retinotopically organized extrastriate areas.

1.3. Evidence from fMRI studies in humans

Several groups of investigators have recently used fMRI to identify the specific regions of visual cortex where neural activity is modulated by spatial attention (reviewed in Posner & Gilbert (1999), Sengpiel & Huebener (1999)). The approach was to delineate the cortical boundaries of the retinotopic visual areas (V1, V2, V3/VP, V4, V7, V8) using recently developed methods (e.g. Sereno et al., 1995; DeYoe et al., 1996; Engel, Glover, & Wandell, 1997b) and then to localize attention-related activity within those areas. In contrast to the ERP evidence suggesting that spatial attention does not modify sensory evoked activity in primary visual cortex, these fMRI studies found clear evidence for modulation of neural activity in area V1 as well as in other retinotopic visual areas during spatial attention (Worden & Schneider, 1996; Tootell et al., 1998; Brefczynski & DeYoe, 1999; Gandhi, Heeger, & Boynton, 1999; Martinez et al., 1999; Somers, Dale, Seiffert, & Tootell, 1999). The general design of these studies was to present concurrent sequences of stimuli to two or more locations within the visual fields and to attend to stimuli at each of the locations in turn on different runs. Modulations of V1 activity were observed during a variety of discriminative tasks, including judgements of line orientation (Tootell et al., 1998), movement velocity (Gandhi et al., 1999), rotational direction of movement and letter identity (Somers et al., 1999), color/orientation conjunctions (Brefczynski & DeYoe, 1999) and shape/letter orientation (Worden & Schneider, 1996; Martinez et al., 1999). Several additional studies have reported changes in V1 activity in active-passive task comparisons that might involve general arousal differences (Shulman et al., 1997; Buchel et al., 1998; Watanabe et al., 1998a; Watanabe et al., 1998b; Jancke, Mirzazade, & Shah, 1999).

In these fMRI studies, attention-related increases in neural activity in both striate and extrastriate areas were found to occur in circumscribed zones that corresponded closely to the retinotopic projections of the attended stimulus location (Kastner, DeWeerd, Desimone, & Ungerleider, 1998; Tootell et al., 1998; Brefczynski & DeYoe, 1999; Martinez et al., 1999; Somers et al., 1999). In other words, the effect of spatial attention was to enhance neural activity in the same retinotopic areas that were activated during passive viewing of the task stimuli. This pattern was observed for visual areas V1, V2, V3/VP, V3A and V4, as well as more anterior retinotopic areas, with the extent of activated cortex increasing progressively in higher-tier areas. It was also found that neural activity was actually reduced below baseline levels in retinotopic areas corresponding to non-attended zones of the visual fields (Tootell et al., 1998; Smith, Singh, & Greenlee, 2000). This suggests that spatial attention facilitates activity in neural populations receiving input from stimuli at attended locations while suppressing neural activity in cortical regions representing unattended locations. What is not clear from these fMRI studies, however, is whether the topographically organized changes in activation observed during spatial attention represent a modulation of sensory evoked activity or a change in baseline firing rates that are not stimulus driven (cf. Luck et al., 1997; Chawla, Rees, & Friston, 1999; Kastner, Pinsk, DeWeerd, Desimone, & Ungerleider, 1999; Hopfinger et al., 2000).

1.4. Present experiment

In a recent study (Martinez, 1999; Martinez et al., 1999) we combined ERP recordings with fMRI to investigate the time course of enhanced neural activity in different visual areas during spatial attention. The aim was to localize attention-related changes in neural activity to specific retinotopic areas that were mapped onto the reconstructed cortical surface using the method of Sereno et al. (1995). The attentional task required subjects to discriminate a target from surrounding distractors in stimulus arrays that were flashed in random order to the right or left of fixation at a rate of around 2/s (see Fig. 1). A central arrow indicated which side was to be attended in successive 20-s blocks. In the fMRI session, increased neural activity was demonstrated in retinotopic visual areas V1, V2, V3/VP, and V4v of the hemisphere contralateral to the attended visual field. These attention-related activations were produced in discrete dorsal and ventral zones of these visual areas corresponding to the stimulus position spanning the horizontal meridian. In a separate ERP recording session using the same task and subjects, stimulus arrays in the attended field elicited

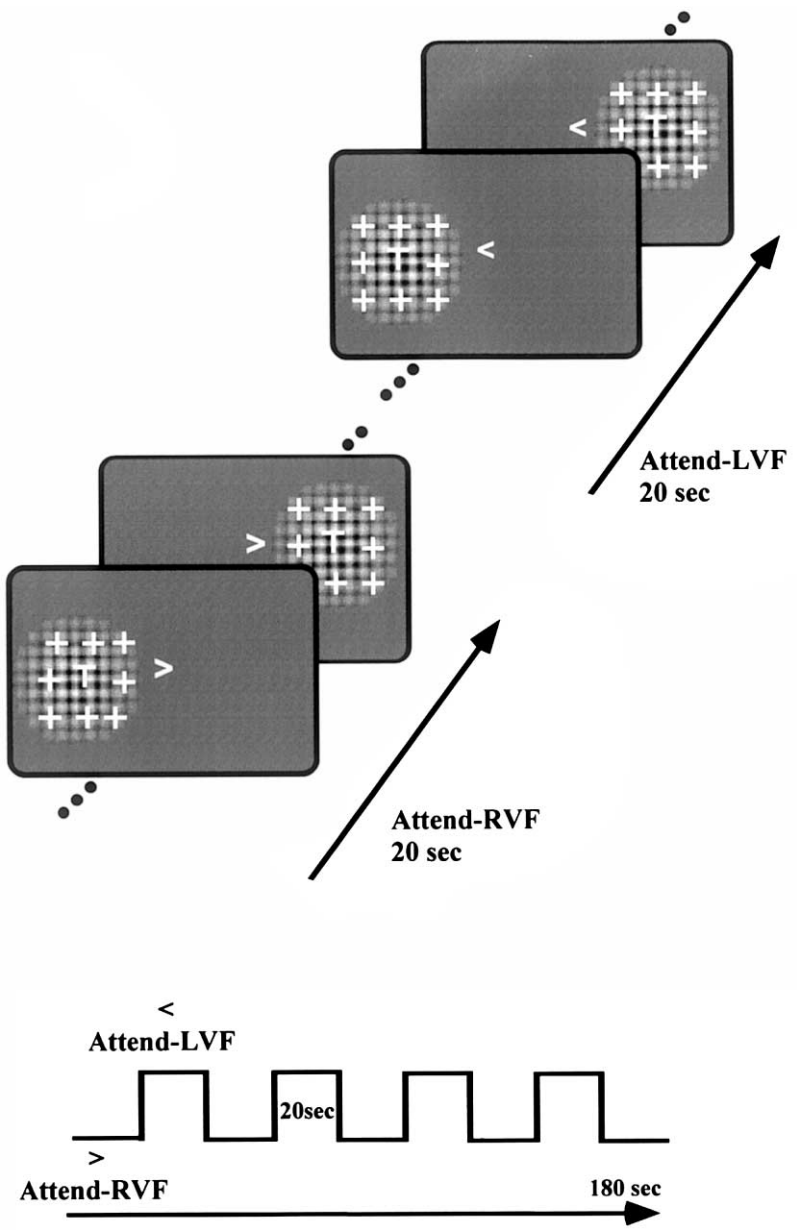

Fig. 1. Experimental stimuli and design. Each stimulus consisted of a 3×3 array of plus signs superimposed on a sinusoidally modulated checkerboard pattern. The center element of each array was either an upright 'T' (standard) or inverted 'T' (target). Stimuli were presented in random sequence to either the left (LVF) or right (RVF) visual field. A central arrow indicated the to-be-attended side and also served as the fixation point. The direction of the arrow alternated between the RVF and LVF every 20 s during each run of 180 s.

enhanced P1 and N1 components over the contralateral occipital scalp as in previous studies. The increased P1 activity was well-modeled by two successively active dipolar sources, the first in dorsal extrastriate cortex during the range 72–104 ms and the second in the ventral, posterior fusiform gyrus over the interval 104–136 ms. Once again the earlier C1 component (onset at 50 ms) did not change as a function of spatial attention, and its dipolar source was localized to the calcarine fissure. We considered two possible explanations for this apparent discrepancy between the fMRI evidence for V1 activation and the lack of any attention effect on the early C1 component. The first was that the attentional modulation of striate cortex activity occurred at a latency longer than that of the initial evoked response represented by the C1, perhaps as a consequence of delayed feedback of enhanced visual signals back to V1 from higher extrastriate areas. An alternative explanation would be that the V1 activity observed with fMRI might represent a top-down attentional 'bias signal' that produced a sustained increase in neuronal activity in V1 but did not modulate the initial stimulus-evoked response.The present paper describes several aspects of the Martinez (1999) study that were not included in the initial report of Martinez et al. (1999). First, additional fMRI data is presented from a passive condition in which the subject simply viewed the task stimuli with no task assignment. A quantitative assessment is made of the extent of overlap between the zones of visual cortex activated by passive stimulation and the zones where attention-related modulation occurred. Second, the estimated locations of the neural sources of the attention-invariant C1 component and the early positivity (P1) enhanced by attention were coregistered with clusters of fMRI activation to provide converging evidence for the validity of the source localization algorithm. Third, a new model of the dipolar sources of the attention-related ERP changes over a more extended time range provides evidence for a long-latency modulation of neural activity in area V1 during spatial attention.

2. Methods

2.1. Subjects

Nineteen neurologically normal subjects (13 female, age range 18–41 years) were paid to participate in the ERP experiment. A subset of six of these subjects (five female, age range 23–41 years) additionally participated in the fMRI study. All subjects were right-handed, as assessed by a brief questionnaire and had normal or corrected-to-normal vision.

2.2. Stimuli and task

The same stimuli and task were used in both the fMRI and ERP attention experiments. The stimuli consisted of 3×3 arrays of crosses superimposed on sinusoidally modulated black and white checkerboard patterns (2 cycles per degree) (Fig. 1). On most trials the central position of the 3×3 array was an upright 'T' shape that inverted on 7% of the presentations. Subjects indicated detection of these 'target' (inverted 'T') arrays by making a manual button press response. Stimuli were presented in randomized order to either the left (LVF) or right (RVF) visual field at a fairly rapid presentation rate (SOAs varying between 400 and 600 ms). Stimulus durations were brief (100 ms) in order to maximize the focusing of attention. Stimuli were delivered on a gray field that was equal in luminance to that of the mean value of the checkerboard patterns. Each stimulus subtended 5.5° of visual angle, and the innermost edge appeared 1.7° to the left or right of fixation.

While maintaining fixation on a central arrow, subjects were instructed to covertly attend to either the LVF or RVF and to press a button upon detection of the infrequent target stimuli appearing in the attended visual field. The to-be-attended side alternated every 20 s as indicated by the direction of the central fixation arrow that remained present on the screen at all times. Each experimental run lasted 3 min and consisted of four attend-LVF sequences and five attend-RVF sequences (20 s each). Subjects received four such runs with fMRI scanning and eight runs with ERP recordings. Each subject received about 320 stimuli in each field/condition in the fMRI experiment and 640 in the ERP experiment.

In addition, to assess passive sensory processing in cortical visual areas, subjects participating in the fMRI portion of the experiment were given a single run of visual stimulation under conditions where no task was assigned and no behavioral responses were required. These passive runs consisted of presentations of the same stimuli at the same rate, but the stimuli were now delivered unilaterally in alternating 20-s blocks to the LVF or to the RVF while subjects maintained fixation on a central cross. (In this study the average rate of stimulus presentation to each visual field was twice as fast in the passive as in the active attention condition. While this difference may produce different refractory/habituation effects on the neural responses in the two conditions, the main point of the active/passive comparison was to examine the anatomical correspondence of the activations rather than their relative magnitudes. Indeed because the rate dependency of the passive response and the attentional modulations may well be different, there is no principled a priori way to adjust the rates to produce equal amplitude modulations.)

2.3. fMRI scanning

Functional imaging was carried out on a Siemens VISION 1.5T clinical scanner equipped with gradient echo-planar capabilities and a standard-equipment circularly polarized head coil optimized for brain imaging. Blood oxygen level dependent (BOLD) images were acquired with an echo planar imaging sequence (TR = 2500 ms, TE = 64 ms, flip angle = 90°) in the coronal plane (2.5×2.5 mm in-plane resolution). Seventy-four repetitions on each of ten 5 mm slices were acquired during each three minute run; the first two repetitions were not used in data analysis. Imaging began at the occipital pole and extended anteriorly. For anatomical localization, high-resolution ($1 \times 1 \times 1$ mm) T1-weighted images of the whole brain were acquired using a 3-D Magnetization Prepared Rapid Gradient Echo sequence (TR = 11.4 ms, TE = 4.4 ms, flip angle = 10°). Both anatomical and BOLD-weighted images were transformed into the standardized coordinate system of Talairach and Tournoux (1988).

Subjects were selected for participation in fMRI scanning on the basis of their ability to maintain steady visual fixation as assessed by electro-oculographic recordings during the ERP recording sessions. Additionally, during fMRI scanning, eye position was monitored continuously using an infrared sensitive video camera system having a sensitivity of $\pm 0.5°$ of visual angle. Runs with detectable eye movements were discarded and repeated. Stimuli were back-projected onto a screen at the foot of the magnet bore and were viewed via a mirror attached to the head coil. The time sequence of BOLD-weighted echo planar images was analyzed with AFNI software (Cox, 1996). The raw time series of signal strength were first averaged individually for each subject over the four separate runs following in-plane motion correction, and then a group average was obtained by averaging the time series data (without normalization) over all subjects. Changes in signal strength related to the experimental manipulations were quantified by correlating the signal strength time series with a sequence of phase-shifted trapezoids representing the alternating conditions in the block design of the experiment (either attend-RVF versus attend-LVF or passive presentations to the RVF versus to the LVF). Linear drift was removed from the time series using Gram–Schmitt orthogonalization.

The significance of attention-related and passive-stimulation activations was assessed using a region of interest (ROI) analysis. Anatomical regions showing activations in both conditions were identified in four pilot subjects (not included in the present data set), and a single, large-volume (28 ml) ROI was defined within the occipital cortex. Included in the ROI were the regions of the calcarine fissure, lingual gyrus, collateral sulcus, middle occipital gyrus and neighboring sulci, and the posterior fusiform gyrus. Significance levels of activation were determined using a Bonferroni correction based on the number of ROI voxels. Activations were considered significant for those voxels that correlated with the direction of attention or field of passive stimulation with $r > 0.5$, $P < 0.02$ (corrected). To minimize the likelihood of falsely detecting spurious activations, only significantly correlated voxels occurring in clusters of four or more (comprising an activation area of 125 mm^3 or greater) were considered in subsequent analyses. This cluster size was chosen based on iterative Monte Carlo simulations using the program AlphaSim. AlphaSim estimates the statistical power (the probability of a true detection) by iteration of the process of random image generation, Gaussian filtering (to simulate voxel correlation), thresholding, and tabulation of cluster size frequencies. The probability that clusters of four or more voxels with correlations greater than 0.5 occurred by chance was estimated to be $< 4\%$ ($P \leq 0.04$).

2.4. Retinotopic mapping of visual areas

In a separate fMRI scanning session BOLD-weighted images were obtained during two separate scans while subjects viewed either a slowly rotating checkerboard wedge or a dilating checkerboard ring. Polar angle (angle from the center-of-gaze) and eccentricity (distance from the center-of-gaze) maps were calculated from the periodic excitation produced by these two stimuli. From these paired scans visual field sign maps were generated in order to delineate the borders of retinotopically organized visual areas based on whether they contain a mirror-image, or non-mirror image representation of the visual field (see Sereno et al. (1995) for details).

During the same scanning session two whole-head high resolution ($1 \times 1 \times 1$ mm) structural image sets were obtained from each participant. These two data sets were averaged and used for reconstruction of each subject's cortical surface. The folded cortical surface was inflated and the occipital lobe was completely detached and flattened using the algorithm of Sereno et al. (1995). The echo-planar volume data sets containing the visual field sign maps as well as the cross-correlation maps from the attention and passive stimulation experiments were projected onto the rendered and flattened cortical surface of each individual.

2.5. ERP recordings

Subjects sat in a dimly lit sound-attenuated and electrically shielded room while viewing stimuli presented on a 24 in. video monitor at a viewing distance of 70 cm. Recordings were made from 41 scalp electrode sites using a modified 10–20 system montage.

Standard 10–20 sites were Fz, F3, F4, F7, F8, Cz, C3, C4, Pz, P3, P4, O1, O2, T3, T4, T5, T6 and the left mastoid. Additional intermediate sites were IPz, INz, IN3, IN4, IN5, IN6, PO1, PO2, TO1, TO2, CP1, CP2, CT5, CT6, FP1, FP2, FC1, FC2, FC5, FC6, C1, C2, C5, and C6. All scalp channels were referenced to an electrode at the right mastoid. Horizontal eye movements were monitored with two bipolar electrodes at the left and right outer canthi. Blinks were recorded with an electrode below the left eye, which was also referenced to the right mastoid.

The EEG from each electrode site was digitized at 250 Hz with an amplifier bandpass of 0.01–80 Hz (half amplitude low- and high-frequency cutoffs, respectively) and stored for off-line averaging. Computerized artifact rejection was performed prior to signal averaging in order to eliminate epochs in which deviations in eye position, blinks, or amplifier blocking occurred. In addition, ERPs to standard stimuli that were preceded by a target stimulus within 1000 ms or followed by a target within 200 ms were eliminated in order to avoid contamination of the average by ERPs related to target detection (e.g., the P300) or motor responses. On average, 17% of the trials were rejected due to a combination these artifact sources. Blinks and eye movements were the most frequent cause for rejection.

ERPs time-locked to the task stimuli were averaged separately according to field of stimulus presentation (LVF or RVF) and whether they were attended or unattended. Each average was based on 500–600 stimuli for each subject. Due to the fast presentation rate used in this experiment it was necessary to remove the overlap between ERPs elicited by successive stimuli. This was done using the ADJAR technique (Woldorff, 1993) for each subject's data. This procedure subtracts the estimated overlap elicited by previous and subsequent stimuli from the averaged ERP waveform such that the resultant waveform consists of the evoked activity for the current stimulus alone. After applying the ADJAR correction, the averaged ERPs were low-pass filtered by convolving the waveforms with a Gaussian function. ERPs were grand-averaged across subjects without normalization.

Prominent ERP components were quantified in terms of mean voltage amplitudes within specified latency windows with respect to a 100 ms pre-stimulus baseline. Mean amplitudes of the C1 (50–80 ms), P1 in its early (72–104 ms) and late (104–136 ms) phases, the posterior N1 (150–180 ms) and the anterior N1 (130–160 ms) were subjected to repeated measures analysis of variance (ANOVA) with factors of attention (same stimulus when attended and unattended), visual field (left and right), electrode site (mirror-image pairs of recording sites at which each component showed maximal amplitude), and hemisphere (left and right). The *P*-values were adjusted for heterogeneity of variance and covariance by the Greenhouse–Geisser ε coefficient.

Additional averages were obtained on a long time base in order to verify that subjects eyes did not slowly drift toward the attended stimuli. These averages were made by time-locking the ERPs to the onset of each directional cue (left- and right-pointing arrows, separately) and averaging the HEOG data over the subsequent 20 s (the duration of each directed attention block). Subjects showing deviations from fixation of greater than one degree of visual angle, corresponding to 10 μV, (Hawkins et al., 1990) during the course of each 20-s block were not included in further analyses.

2.6. Modeling of ERP sources

The exact location of each electrode site was determined by means of a Polhemus spatial digitizer which recorded the three-dimensional coordinates of each electrode and of three fiducial landmarks (the left and right preauricular points and the nasion). A computer algorithm was used to calculate the best-fit sphere that encompassed the array of electrode sites and to determine their spherical coordinates. The mean scalp location of each site was estimated by averaging each electrode location across all subjects. These averaged values were used for the topographic mapping and source localization procedures. In addition, individual spherical coordinates were related to the corresponding digitized fiducial landmarks and to fiducial landmarks identified on whole-head MRIs of seven subjects. In this manner, the locations of the estimated dipoles could be related to individual brain-skull anatomy.

Estimation of the dipolar sources of ERP components was carried out using the brain electrical source analysis (BESA) algorithm as described previously (Scherg, 1990; Clark et al., 1995; Anllo-Vento, Luck, & Hillyard, 1998). The general strategy was to fit dipoles (either singly or in pairs) to each ERP component in sequence over a time range when its scalp distribution was relatively stable. Dipole locations and orientations were adjusted iteratively to minimize the residual variance between the scalp voltage topography of the forward solution from the model and the scalp topography of the actual data. The results of two different modeling approaches are considered here. In the first, reported by Martinez et al. (1999), modeling of the unattended C1 component and the P1 attentional modulation was carried out jointly on waveforms elicited by RVF and LVF stimuli. In the second approach, the C1, P1, and N1 components were modeled in the ERPs to RVF and LVF stimuli considered separately, with the attended and unattended waveforms for each field modeled jointly. For both modeling strategies it was found that the resulting dipole locations were little affected by using different symmetry constraints or different starting positions in the dipole fitting procedure.

To estimate the dipole locations with respect to brain anatomy, the dipole coordinates of the BESA model calculated from the grand average ERP distributions were projected onto the MRIs of individual subjects as described above. After establishing the line between the anterior and posterior commissures on each subject's MRI scan, the 3-dimensional coordinates of each dipole in the group-averaged BESA model were transformed to coordinates of the Talairach and Tournoux (1988) atlas. To obtain an estimate of the average locations of each dipole across the group, the mean values of the Talairach coordinates of each dipole were calculated over the 6 subjects whose MRIs were available (Clark & Hillyard, 1996; Anllo-Vento et al., 1998). These dipole positions could then be compared in Talairach space with clusters of fMRI activations as determined from the AFNI analysis.

3. Results

3.1. fMRI results

Sensory-related activations produced by passive visual stimulation were observed in several striate and extrastriate visual cortical areas in the hemisphere contralateral to the stimulated visual field. These areas included the calcarine fissure, the lingual and fusiform gyri, and the middle occipital gyrus and neighboring sulci (Fig. 2). In order to localize these sensory-evoked activations to specific visual areas, the passive viewing maps from each individual were projected onto the flattened surface renditions of their occipital lobes and coregistered with the corresponding field sign maps of the visual areas (Fig. 3). The majority of subjects had well-defined clusters of significant activation in all the retinotopic areas (V1, V2, V3/VP, V3A and V4v) as well as weakly retinotopic regions of the middle occipital gyrus anterior to area V3A and in the posterior fusiform gyrus anterior to area V4v. These sensory-related activations were produced in discrete zones of retinotopically organized cortex corresponding to the eccentricity of the stimuli in the visual field. Because the stimuli spanned the horizontal meridian, sensory-related increases in the MR signal were produced in both upper and lower visual field representations in the ventral and dorsal cortical areas, respectively. Table 1 lists the Talairach coordinates of the clusters of activation in each visual area during passive viewing, averaged across subjects.

During the spatial attention condition, subjects correctly detected $71 \pm 8\%$ of the targets in the attended visual field. Significant fMRI activations correlated with the direction of attention were observed in the calcarine fissure, lingual and fusiform gyri, middle occipital gyrus, and posterior parietal cortex, all in the hemisphere contralateral to the attended visual field (Fig. 2). Projections of the individual attention-related activity maps onto the flattened occipital surface showed significant increases in the BOLD signal with attention in area V1 in all subjects and in areas V2, V3/VP and V4v in the majority of subjects (Fig. 3 and Table 1). Most subjects also showed significant activations in the middle occipital gyrus and adjacent sulci anterior to area V3A, in the posterior fusiform gyrus anterior to area V4v, and in the posterior parietal cortex.

Figs. 2 and 3 show a high degree of correspondence between the areas activated by passive viewing and those modulated in the spatial attention task. In addition, Table 1 indicates that the Talairach coordinates of the activation clusters in the two conditions are very similar. Indeed, of the brain voxels that were significantly active during passive viewing, 42% were also activated during the attention conditions. Conversely, 60% of the voxels showing significant modulation during spatial attention were also significantly activated during passive viewing. This concordance was reflected in a highly significant $\chi^2 = 62{,}267$ ($P < 0.0001$).

3.2. ERP results

In the ERP recording runs, subjects correctly detected $81 \pm 7\%$ of the targets in the attended visual field. (The somewhat lower detection rate found during fMRI scanning (71 vs. 81%) was most likely attributable to the less comfortable and more distracting setting inside the bore of the magnet, together with a slightly less sharp, back-projected visual image. Stimulus arrays in the attended visual field elicited ERPs with enlarged positive P1 (onset at 70–75 ms) and negative posterior N1 (onset at 130–140 ms) components over the contralateral occipital scalp (Fig. 4). Significant amplitude increases with attention were found for both the early (72–104 ms) and late (104–136 ms) phases of the P1 ($F(1,18) = 8.9$, $P < 0.01$, and $F(1,18) = 39.4$, $P < 0.001$, respectively) and for the occipital N1 ($F(1,18) = 15.0$, $P < 0.002$). In addition, a broad centrofrontally distributed negativity (anterior N1) was significantly larger in the attended waveforms ($F(1, 18) = 6.9$, $P < 0.02$). Although these attention effects were generally larger over the hemisphere contralateral to the attended visual field, the interaction of visual field, hemisphere, and attention only reached significance for the early phase of the P1 ($F(1,18) = 6.6$, $P < 0.02$). There were no significant main effects of visual field or of hemisphere on any of these components.

In contrast, the amplitude of the earlier C1 component (onset at 50–60 ms) did not vary significantly with attention ($F(1,18) = 3.6$, N.S.). At posterior sites the measured amplitude of the C1 was either not affected

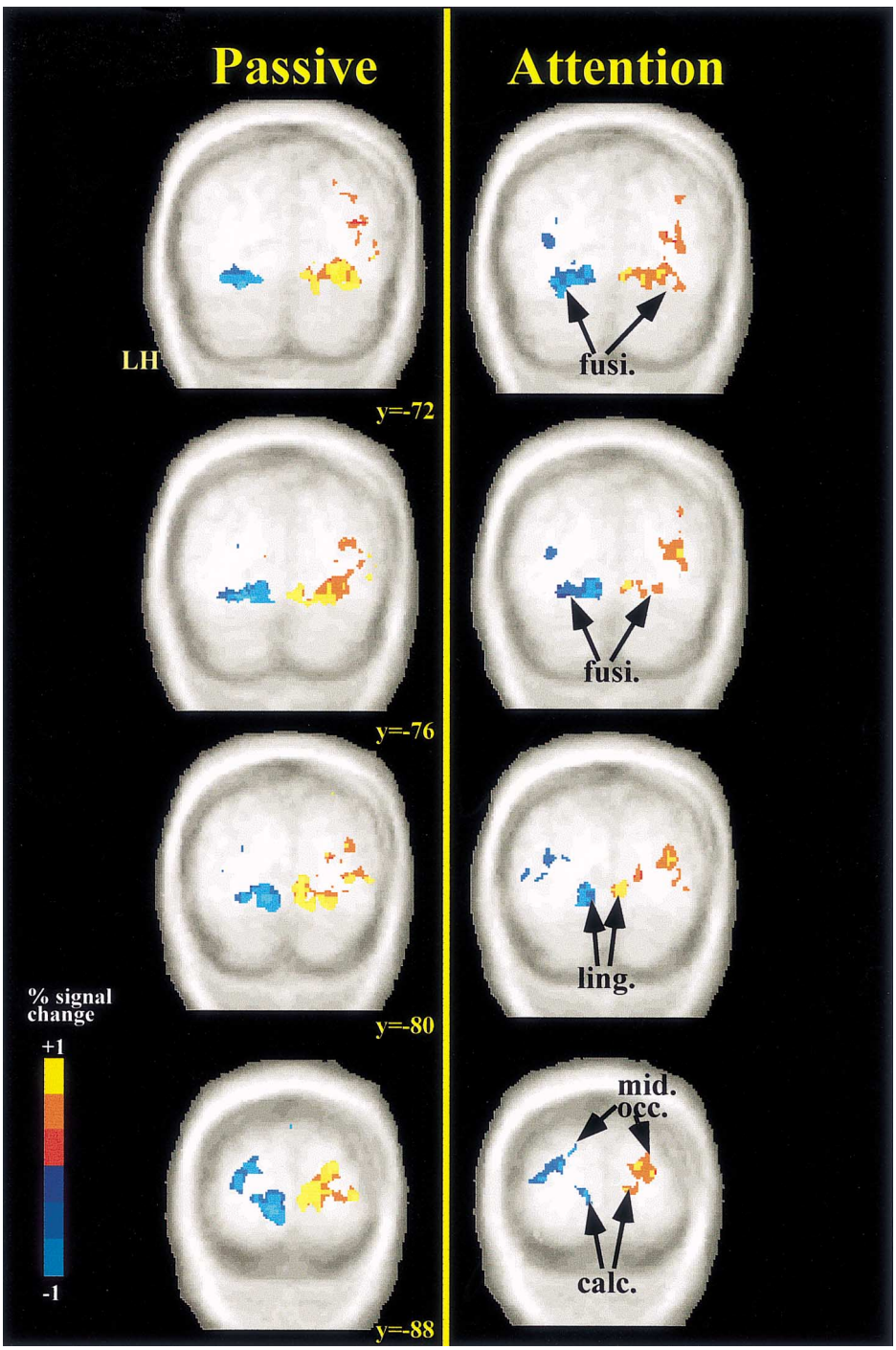

Fig. 2. Grand-averaged fMRI activations over six subjects resulting from passive stimulation (left) and from spatial attention (right). Activations are superimposed on four representative anatomical slices averaged across the six subjects. Talairach coordinates (y-values) of each slice are indicated. In this and all figures the left hemisphere appears on the left. Intensity of colored regions reflects percentage signal change of significantly activated areas. Pixels with a time course of activation positively correlated with the task design (i.e., showing greater signal strength during LVF stimulation in the passive runs or during attend-LVF in the attention runs) are shown in red-to-yellow scale. Pixels showing a negative correlation (i.e., greater activation during RVF stimulation or attend-RVF) are shown in dark-to-light blue scale. Only pixels correlating at $r > \pm 0.5$ ($P < 0.02$, corrected) are shown. Similarly localized contralateral activation foci were seen in the passive and attention conditions in the calcarine fissure (calc.), lingual gyrus (ling.), posterior fusiform gyrus (fusi) and middle occipital gyrus (mid. occ.).

by attention (for LVF stimuli) or was actually reduced in amplitude (for RVF stimuli) due to overlap with the concurrent ipsilateral P1 attention effect. At the Cz site where the C1 distribution did not overlap with that of the P1, there was no change in C1 amplitude as a function of attention (Fig. 4).

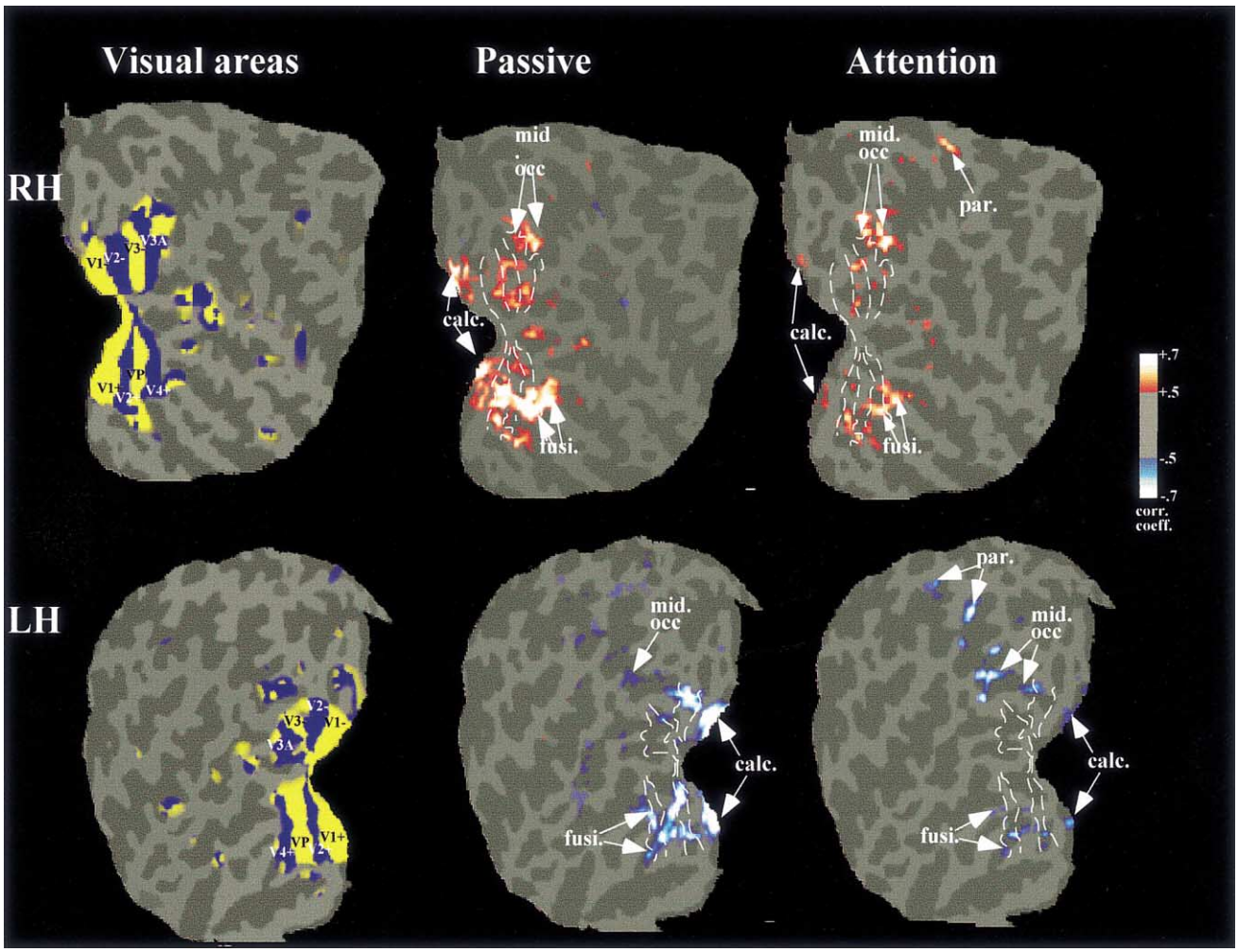

Fig. 3. Sensory-based and attention-related activations projected onto the flattened occipital cortex of a representative subject. The boundaries of the retinotopic areas (V1, V2, V3/VP, V3A and V4v) of each hemisphere were determined by calculating the visual field sign after mapping eccentricity and polar angle. As in Fig. 2, sensory-related and attention-related activations were determined by cross-correlating pixel time courses with the alternating task design. Zones of increased neural activity during passive stimulation or attention to the LVF are shown in red-yellow scale, and foci of increased neural activity during stimulation of/attention to the RVF are shown in blue. Dotted lines on activation maps are boundaries of visual areas as determined by this subject's field sign maps. Abbreviations are as in Fig. 2.

Table 1
Talairach coordinates of activation clusters during passive visual stimulation and during spatial attention[a]

	V1	V2	VP	V4v	Fusi.	
Ventral						
RH: Passive	9, −89, −2 (6)	8, −81, −3 (6)	12, −75, −7 (6)	21, −63, −13 (6)	30, −63, −13 (6)	
RH: Attention	7, −88, 0 (6)	7, −78, −3 (5)	9, −74, −8 (5)	19, −70, −11 (4)	33, −61, −13 (4)	
LH: Passive	−8, −91, −5 (6)	−9, −81, −6 (4)	−16, −76, −9 (6)	−26, −71, −15 (4)	−29, −64, −7 (5)	
LH: Attention	− 9, −90, −5 (4)	−12, −79, −8 (6)	−16, −75, −7 (6)	−26, −76, −11 (5)	−31, −60, −11 (6)	
	V1	V2	V3	V3A	Mid. occ.	Post. par.
Dorsal						
RH: Passive	8, −88, 6 (5)	8, −85, 4 (6)	20, −90, 11 (6)	29, −82, 16 (6)	25, −83, 18 (4)	–, –, – (0)
RH: Attention	7, −89, 1 (6)	7, −84, 5 (3)	21, −88, 13 (5)	24, −81, 19 (2)	27, −75, 13 (4)	28, −49, 57 (3)
LH: Passive	−10, −91, 3 (4)	−9, −86, 4 (4)	−18, −88, 12 (5)	−28 −83, 15 (6)	−29, −77, 19 (5)	–, –, – (0)
LH: Attention	−8, −91, 0 (6)	−10, −85, 0 (5)	−22, −85, 14 (5)	–, –, – (0)	−29, −75, 19 (5)	−29, −55, 50 (3)

[a] Mean co-ordinate values are given for centroids of clusters within each visual area in the ventral and dorsal cortical divisions of the right (RH) and left (LH) hemispheres. The number of subjects (out of six) showing significant ($P<0.02$ corrected) activations in each area is given in parenthesis.

The voltage topography of the P1 attention effect (attended minus unattended ERPs in early and late time windows) differed markedly from that of the C1 component (Fig. 5). The unattended C1 was maximally negative over the midline parieto-occipital scalp ipsilateral to the visual field of the eliciting stimulus. In contrast, the distribution of the P1 attention effect was largest over the contralateral occipital scalp, with a secondary ipsilateral focus that was larger for RVF stimuli. The voltage topography of the P1 shifted over time, such that the later phase (104–136 ms) was more ventrally distributed and more widespread over the occipital scalp than the early phase (72–104 ms).

From these grand-averaged scalp distributions the locations of the intracranial generators of the C1 component and the P1 attention effect were estimated by dipole modeling using the BESA algorithm. The initial analysis (reported in Martinez et al. (1999)) modeled the C1 component with a pair of mirror symmetrical dipoles (one in each hemisphere) that were fit jointly to the waveforms elicited by the unattended left-field and right-field standard stimuli over the time interval 50–80 ms. The best fit pair of dipoles accounted for 92% of the variance in the C1's scalp topography. These dipoles were situated within the calcarine fissure as determined by projecting the BESA dipole coordinates of the group average model on to the MRIs of seven individual subjects and then converting the dipole positions to Talairach coordinates. Averaged over all subjects, these coordinates ($x\ y\ z$) were -9, -85, 5 for the left hemisphere dipole and 10, -85, 5 for the right hemisphere dipole. The close anatomical correspondence between these dipole locations for the unattended C1 and the attention-related fMRI activations within the calcarine fissure are shown in Fig. 6.

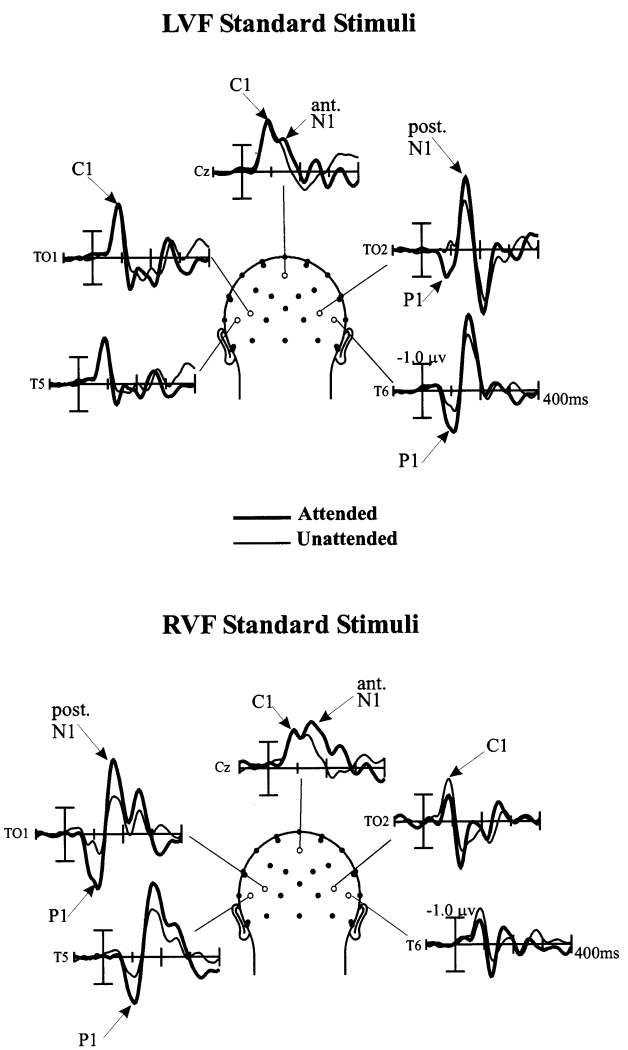

Fig. 4. Grand-averaged ERP waveforms from selected scalp sites in response to standard (non-target) stimuli in the left visual field (LVF, top) and in the right visual field (RVF, bottom). ERPs shown were recorded from electrodes at occipitotemporal (T01/T02), temporal (T5/T6) and midline central (Cz) sites. Other sites are indicted as dots on the head icon.

Two pairs of dipoles that were mirror symmetric in location but not in orientation were required to account for the early and late phases of the P1 attention effects. The scalp topographies of the attentional difference waves (i.e. of the attended minus unattended ERPs) for both left and right field stimuli were fit sequentially over early (72–104 ms) and late (104–136 ms) time windows. The dipole pair fitting the early phase of the P1 attention effect was situated in dorsal extrastriate cortex of the middle occipital gyrus (left hemisphere, -32, -90, 9; right hemisphere, 33, -90, 10). The dipole pair for the late phase was localized to the ventral fusiform gyrus (left hemisphere, -36, -56, -11; right hemisphere, 37, -56, -11). Together, these two dipole pairs accounted for 94.8% of the variance of the scalp distribution of the grand average P1 difference waves in the 72–136 ms interval. Fig. 6 shows the locations of these dipole pairs in juxtaposition with the attention-related activations seen with fMRI. The dipole for the early phase of the P1 corresponded closely with activation foci in area V3 and in neighboring regions of the middle occipital gyrus anterior and lateral to area V3a. The dipoles accounting for the later phase of the P1 attention effect corresponded with fMRI activations in the posterior fusiform gyrus just anterior to area V4v.

3.3. Extended dipole model

To look for evidence of long-latency modulation of striate cortex activity with attention, a new dipole model was constructed using BESA over a longer time interval than the model reported by Martinez et al. (1999). The strategy was to fit dipoles over successive latency windows to both the attended and unattended waveforms concurrently. This was done separately for ERPs to LVF and RVF stimuli, according to the

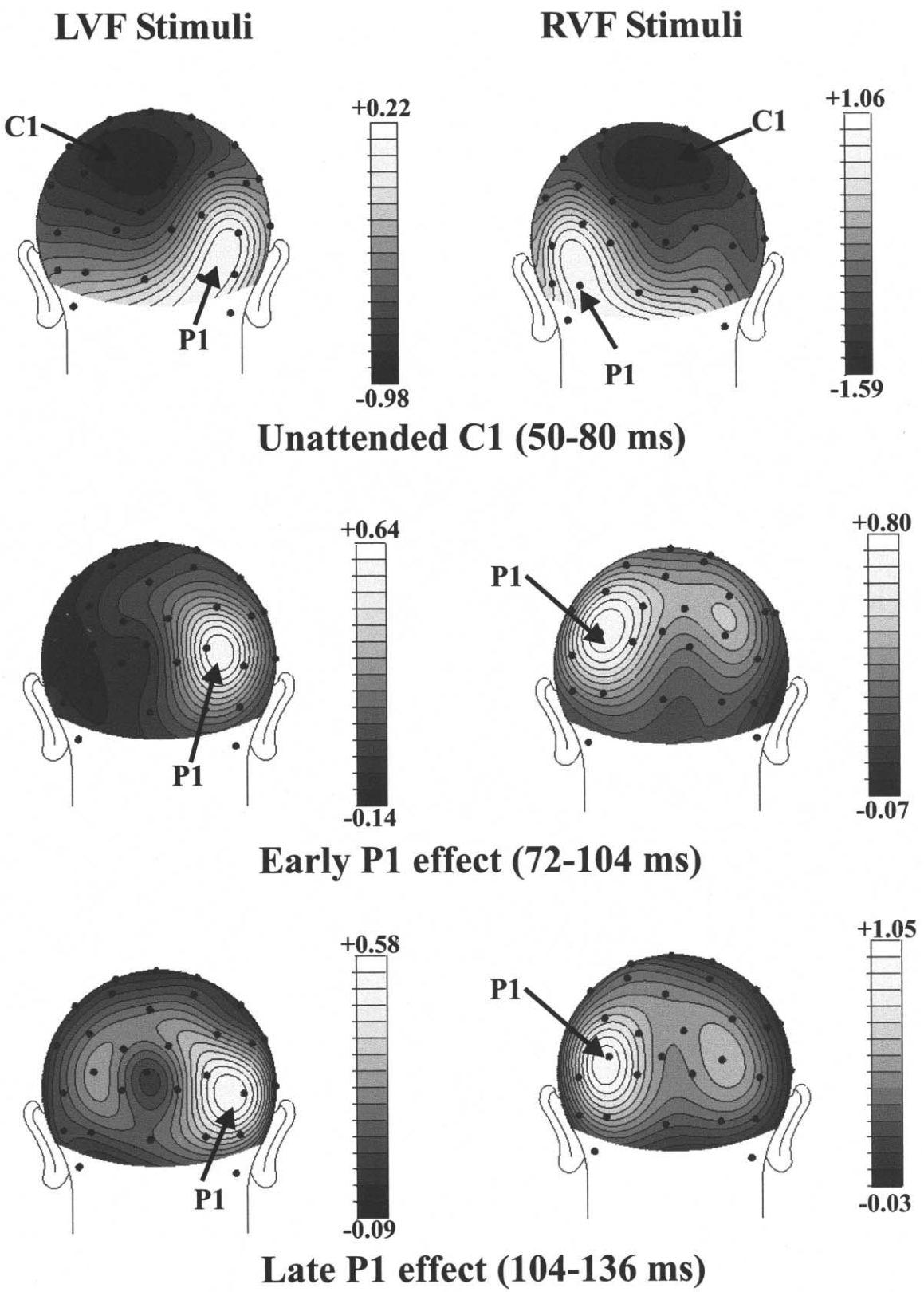

Fig. 5. Voltage topographies of early ERP components. Spline interpolated voltage maps were derived from grand average waveforms. The C1 (top) is mapped as the mean voltage over the time window 50–80 ms for ERPs elicited by unattended stimuli in the left visual field (LVF) and right visual field (RVF). The maps of the P1 attention effects over early (middle) and late (bottom) time windows were derived from the difference waves formed by subtracting the ERPs elicited by standard stimuli when unattended from the ERPs to the same stimuli when attended. Amplitude scales are in microvolts.

following sequence: (1) A single dipole (# 1) was fit to the C1 distribution over the interval 56–80 ms; (2) a mirror symmetric dipole pair (# 2–3) was fit to the early P1 over 80–104 ms; (3) an additional mirror symmetric dipole pair (# 4–5) was fit to the late P1 over 104–136 ms; (4) an additional dipole pair (# 6–7) was fit to the anterior N1 distribution over 108–156 ms; (5) with all dipoles fixed in location, the orientations of dipoles 2–3, 4–5, and 6–7 were adjusted in sequence over the time range 64–176 ms to achieve an optimal fit. (The rationale behind this dipole fitting strategy was as follows: one dipole was fit to the time interval that included the C1, because the lateralized nature of the input to the primary visual cortex predicts a unilateral source in that area. The subsequent P1 intervals were fit with bilateral, mirror symmetric pairs

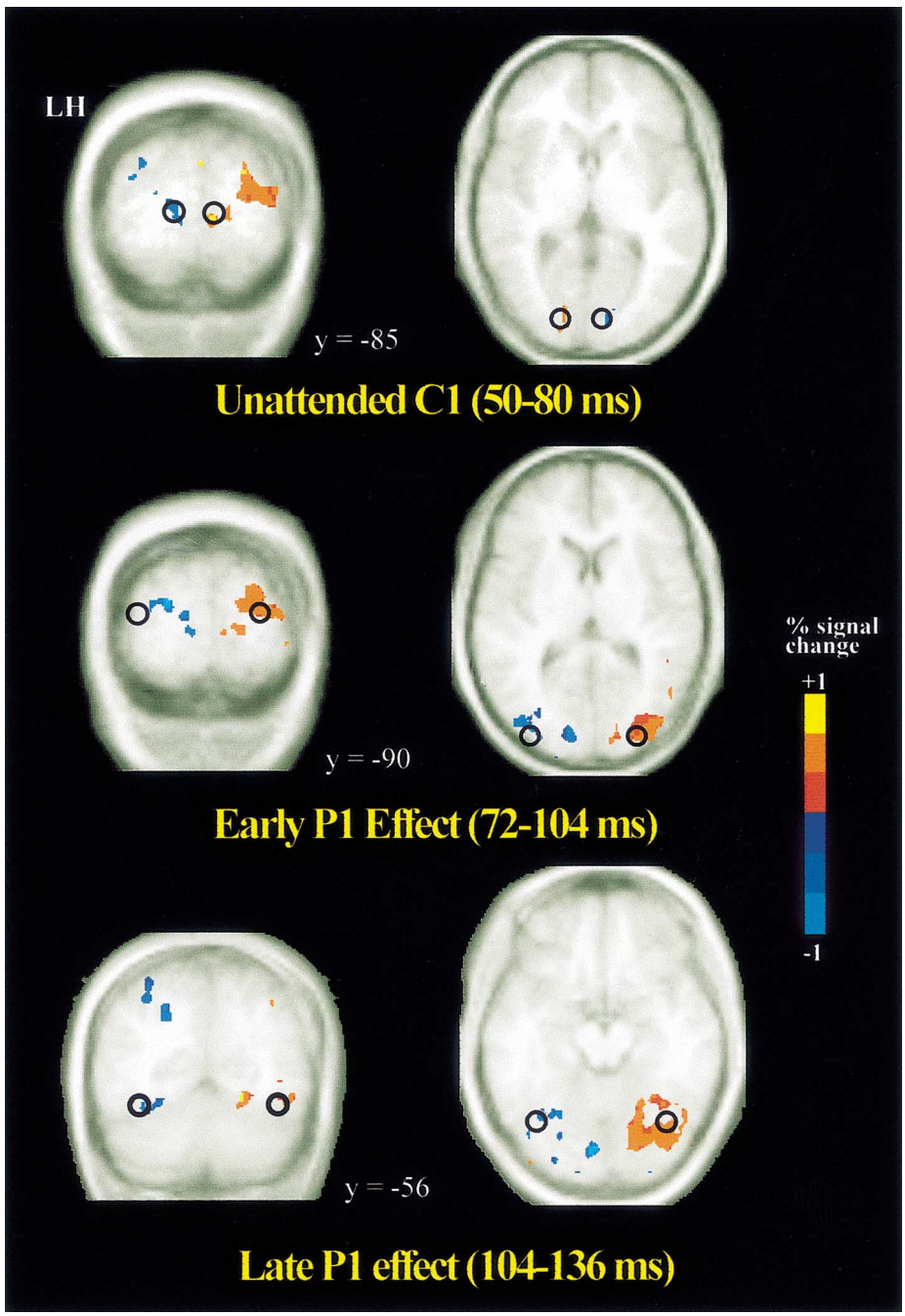

Fig. 6. Superimposition of calculated dipole locations and fMRI activations. Attention-related fMRI activations averaged over six subjects are superimposed on corresponding anatomical images averaged over those subjects. Top: Dipoles calculated for the unattended C1 were co-localized with activations within the calcarine fissure including those in area V1. Middle: Dipoles for the early phase of the P1 attention effect were in close proximity to fMRI activations in dorsal extrastriate areas V3 and middle occipital gyrus. Bottom: Dipoles for the late P1 attention effect were co-localized with ventral fusiform activations.

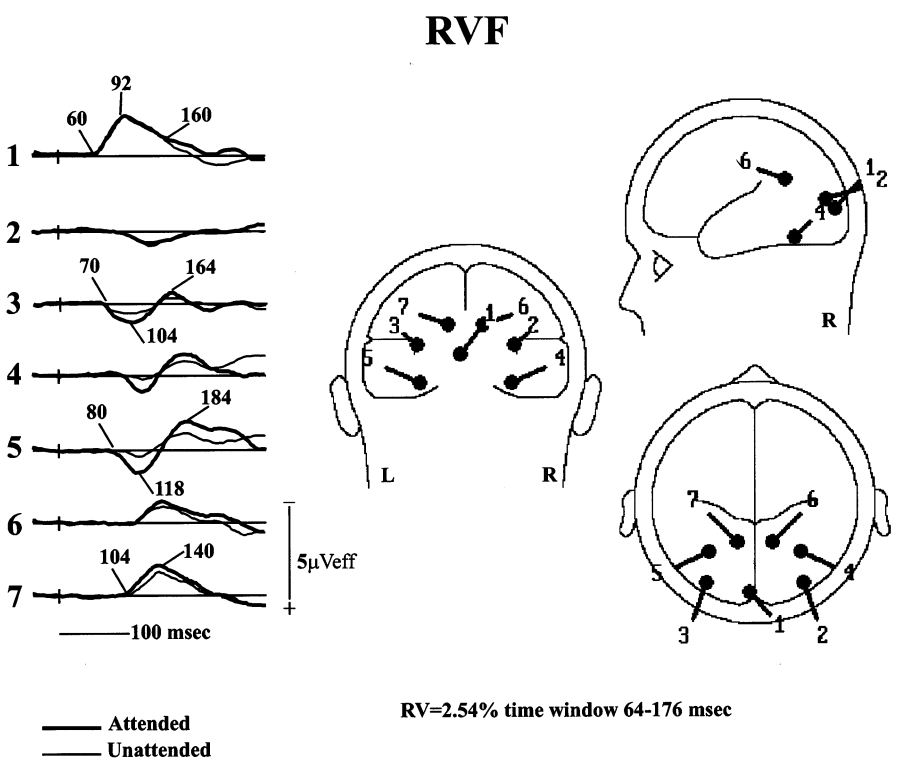

Fig. 7. Sources waveforms (left) and locations (right) of dipoles calculated to best fit the attended and unattended ERP distributions in response to right visual field (RVF) stimuli. Numbers on source waveforms are onset and peak latencies (ms) of various components. See text for details of fitting procedure. The midline occipital dipole (# 1) accounted for the C1 component (60–92 ms) and showed a long latency attention effect starting at 160 ms. Dipole # 3 accounted for the early contralateral P1 (70–104 ms), which was larger in attended waveforms. Dipole # 5 accounted for the late contralateral P1 (80–118 ms). Dipole # 7 accounted for the contralateral anterior N1 (104–140 ms). RV, residual variance.

of dipoles on the basis of previous studies (Mangun & Hillyard, 1995; Clark & Hillyard, 1996; Wijers et al., 1997) showing that the P1 has mirror image foci over the contralateral and ipsilateral occipital scalp, with the ipsilateral focus delayed by some 10–30 ms. This ipsilateral delay, presumably due to transmission across the corpus callosum (Mangun & Hillyard, 1995) can be seen in the source waveforms of Figs. 7 and 8. The N1 also had a bilateral scalp topography and hence was fit with a symmetrical pair of dipoles. Thus, the number of dipoles chosen for the model corresponded to the major topographical features of the ERP scalp distributions.)

The resulting dipole models (Figs. 7 and 8) accounted for 97.9% (RVF) and 97.5% (LVF) of the variance in the scalp voltage topographies over the 64–176 ms interval. As in the model of Martinez et al. (1999), dipole 1 was localized to posterior midline occipital cortex, whereas dipoles 2–3 and 4–5 were situated more laterally in dorsal and ventral occipital areas, respectively. Dipole pair 6–7 was located in superior parietal cortex. Attention-related modulations can be seen in the source waveforms of the extrastriate dipoles that correspond to the early P1/posterior N1 (# 2–3), late P1/posterior N1 (# 4–5), and anterior N1 (# 6–7).

The midline occipital dipole had a source waveform that corresponded to the C1 component over the 60–100 ms interval, with no evidence of any modulation by attention. However, starting at about 160 ms there was an increased negativity in the attended waveform that extended for over one hundred ms. The significance of this negative deflection was evaluated by comparing the attend minus unattend amplitude difference in the source waveforms over successive intervals (152–184, 192–224, and 232–264 ms) with respect to an estimate of the noise variability in this difference measure over the time window -40 to $+60$ ms, before any source activity was evident. This late attention effect was significant in the 152–184 ms interval (LVF, $t(17) = 3.15$, $P < 0.01$; RVF, $t(17) = 1.78$, $P < 0.05$) and became increasingly larger for the later intervals: 192–224 ms (LVF, $t(17) = 3.19$, $P < 0.01$; RVF, $t(17) = 2.45$, $P < 0.02$) and 232–264 ms (LVF, $t(17) = 4.66$, $P < 0.001$; RVF, $t(17) = 4.06$, $P < 0.001$).

4. Discussion

4.1. Attention effects in primary visual cortex

A key result in the fMRI experiment reported here was the robust attentional modulation observed in primary visual cortex. There has been much debate in recent years concerning whether the responses of striate neurons are modulated by spatially directed attention (Posner & Gilbert, 1999; Sengpiel & Huebener, 1999). Worden and Schneider (1996) were the first to report convincing attentional modulation of striate activity in humans using fMRI. Using stimuli similar to those used in the present experiment, these authors found that when target stimuli were surrounded by many confusable distractors (and thus, attention had to be highly focused upon a discrete location in order to reduce interference from competing stimuli) contralateral attention-related modulations were observable in the vicinity of area V1. Other neuroimaging studies using PET, however, failed to find any striate modulations during spatial attention (Heinze et al., 1994b; Mangun, Hopfinger, Kussmaul, Fletcher, & Heinze, 1997; Woldorff et al., 1997). This discrepancy might be accounted for by the hypothesis of Worden and Schneider (1996) that target stimuli must be embedded in a 'cluttered' visual in order to engage primary visual cortex in the selection process. However, it is also possible that the enhanced spatial resolution (and signal-to-noise-ratio) of fMRI relative to that afforded by PET imaging is necessary in order to detect activity within small regions of cortex and, in particular, to dissociate activations in V1 from that occurring in closely neighboring visual areas.

Within the past couple of years, several reports have appeared in which attention effects were demonstrated in retinotopically-defined area V1 (Tootell et al., 1998; Brefczynski & DeYoe, 1999; Gandhi et al., 1999; Somers et al., 1999) including a preliminary version of the present study (Martinez et al., 1999). Like the Worden and Schneider (1996) study discussed above, these recent experiments all utilized designs that made it possible to reliably differentiate attentionally-selective activations from non-selective activations due to changes in arousal. The experimental designs, tasks, and stimuli used in these studies have been very diverse, however, as have the magnitudes of the measured attentional modulations in V1.

In the study of Brefczynski and DeYoe (1999), the stimuli consisted of a dense array of confusable segments. To accurately perform the task subjects had to selectively focus attention on a small region of space (the cued segment) and ignore all competing visual input from the surrounding locations. Similarly, the experiment reported here utilized an array in which target stimuli were surrounded by many confusable

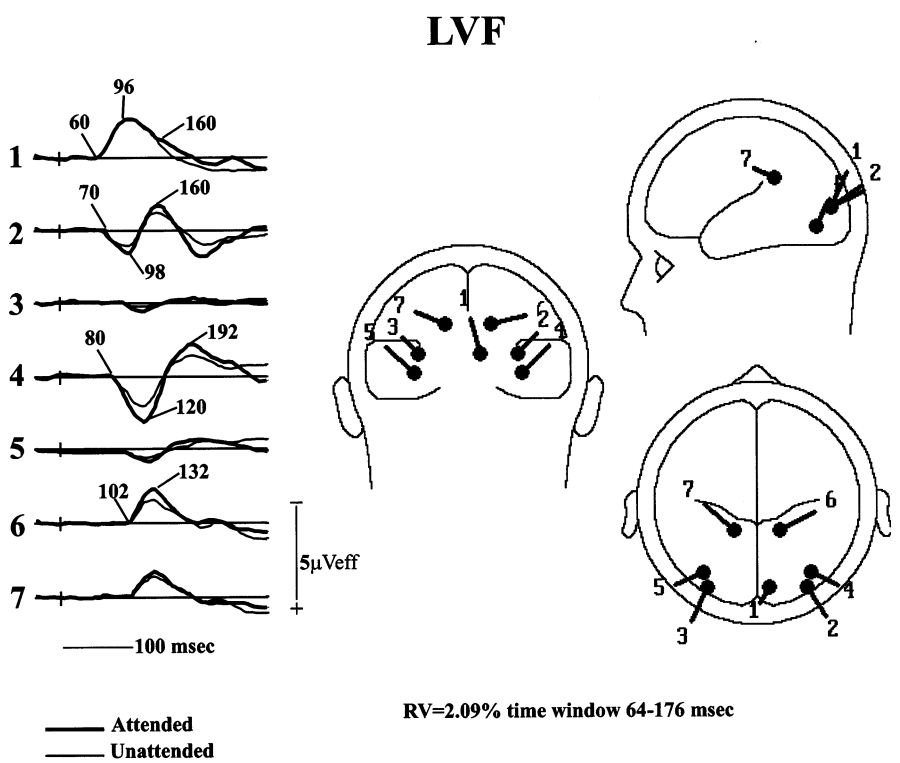

Fig. 8. Same as Fig. 7 for ERPs in response to left visual field (LVF) stimuli. Here, however, dipole #2 accounts for the contralateral early P1 (70–98 ms), dipole #4 accounts for the contralateral late P1 (80–120 ms) and dipole #6 accounts for the contralateral anterior N1 (102-132 ms).

distractors, thus requiring a small and highly-focused attentional spotlight. However, none of the three other studies showing modulations of V1 activity (Tootell et al., 1998; Gandhi et al., 1999; Somers et al., 1999) presented cluttered visual displays. In fact, the design of Tootell et al. (1998) consisted of a relatively sparse visual field (a single bar in each visual quadrant) with highly discriminable targets. The task of Somers et al. (1999) was dissimilar from the rest in that these authors compared foveal versus parafoveal attention to two types of stimuli (letters and rotating gratings), yet their findings of activation in striate cortex was comparable. It appears, therefore, that cluttered visual arrays are not always necessary to produce modulations in striate cortex activity during spatially focused attention.

4.2. The retinotopic organization of spatial attention

One important finding of both the Brefczynski and DeYoe (1999) and Tootell et al. (1998) studies was that the activations resulting from spatially-mediated attention were retinotopically organized according to the spatial positioning of attention within the visual field. Tootell et al. (1998) compared activations resulting from passive stimulation with bar-shaped stimuli with activity maps produced by focused attention to each quadrant. Passive viewing of the target stimuli in each quadrant resulted in a chain-like pattern of activations that extended through each retinotopic visual area. These passive activations were centered at the expected locations corresponding to the parafoveal eccentricity at which the stimuli appeared. In addition, the 'spread' of activation (that is, the thickness of the activation chain) was greater in higher-order retinotopic areas (e.g. V3A) than in lower-tier areas such as V1 and V2, which is consistent with findings from monkey studies showing that receptive field sizes increase progressively going from lower-order areas (e.g. V1) to higher-order retinotopic areas (e.g. V3A).

The correspondence between the activity maps produced by passive stimulus delivery and focused spatial attention in the Tootell et al. (1998) study was, in general, quite close. Attention to a given visual quadrant produced enhanced activations in the sensory representations of the attended location in each of the visual areas. Also, just as the sensory-based activations expanded in the higher, relative to lower, visual areas, so did the attention-related activations. This finding was interpreted by the authors as suggesting that the receptive field mechanisms that underlie spatially-guided attentional selection are similar to those involved in sensory-based processing.

In the present study a good correspondence was also found between areas activated by passive stimulation and those modulated by attention. Indeed, aside from the overall greater amount of activation (both in terms of brain area and signal strength) in the passive stimulation condition, the two maps were virtually indistinguishable from one another. In both cases, activations were observed in both dorsal and ventral extrastriate areas, corresponding to the stimulus location spanning the horizontal meridian. In addition, both the sensory-based activations and the attention-related activations occurred at the expected parafoveal locations corresponding to the representation of the stimulated portion of the visual field. This finding, and those of Tootell et al. (1998) and Brefczynski and DeYoe (1999) support the view that, rather than recruiting a different population of neurons, spatial attention operates to increase the gain of sensory-evoked neural responses (Posner & Dehaene, 1994; Hillyard et al., 1998).

4.3. Attention effects in extrastriate cortical areas

In the present experiment, the observed enhancement of attention-related signals in multiple extrastriate visual areas is consistent with previous neuroimaging studies of spatial attention (Heinze et al., 1994b; Mangun et al., 1997; Woldorff et al., 1997; Kastner et al., 1998; Tootell et al., 1998; Brefczynski & DeYoe, 1999; Gandhi et al., 1999; Hopfinger et al., 2000). These studies have all reported increased blood-flow changes in extrastriate cortical areas in the hemisphere contralateral to the attended visual field.

As in the present report, Somers et al. (1999), Tootell et al. (1998), Kastner et al. (1998) and Brefczynski and DeYoe (1999) found robust attention-related activations in extrastriate areas V2, V4 and in regions extending beyond V4 into the neighboring posterior fusiform gyrus (retinotopic area V8, Tootell et al. (1997)). There is less consistency amongst these studies when considering attention-related activity in other extrastriate visual areas, however, possibly due to the wide range of tasks and stimuli that were used. In the majority of studies (including the present), attentional modulations were observed in ventral occipital area VP as well as in the corresponding dorsal-occipital area V3. Only two of the six studies (Tootell et al., 1998; Somers et al., 1999), however, found attention-related enhancements in area V3A (in both its upper and lower field representations). Interestingly, both of the studies that obtained attention effects in V3A employed an MRI scanner with greater field strength (3T). Perhaps attention-related activity in V3A is not detectable under the considerably lower magnetic fields produced by the 1.5T scanners used in the other studies.

Other cortical areas showing activation related to spatial attention were in V7 (anterior to V3A, near the middle occipital gyrus) (Tootell et al., 1998) and in the human homologue of monkey area MT, (MT+). Two of the studies reviewed here (Tootell et al., 1998; Somers et al., 1999) as well as the present study found

attentional enhancements of activity in area V7 (corresponding to the middle-occipital gyrus in the present experiment). For two of these studies (the present and Tootell et al. (1998)), these activations were very robust and consistent among individual subjects. Area MT+ was also modulated by attention to the contralateral visual field in the studies of Gandhi et al. (1999) and Tootell et al. (1998). The task used by Gandhi et al. (1999) used moving gratings as the attended stimuli and thus was specifically designed to investigate attention effects in MT+. Although it may seem surprising that Tootell et al. (1998) obtained attention-related modulations of MT+ using stationary targets, these authors pointed out that the occasional shifts between horizontal and vertical bar orientations produced a subtle perception of rotational motion. Furthermore, human MT+ reportedly responds well to flickering stimuli (Tootell et al., 1995) similar to those used by Tootell et al. (1998).

In addition to the extrastriate activations described above, robust attention-related signals were obtained in the contralateral superior parietal cortex of some subjects in an area bordering the intraparietal sulcus. This activation site corresponds closely with that reported by several authors (Kastner et al., 1999; Corbetta, Kincade, Ollinger, McAvoy, & Shulman, 2000; Hopfinger et al., 2000) during tasks requiring sustained covert attention to spatial locations in the peripheral visual fields. In contrast, passive visual stimulation did not produce any significant activations in parietal cortex, suggesting that the observed attention-related activity most likely reflects the engagement of a top-down attentional control circuitry that orchestrates the facilitation of attended inputs in extrastriate visual cortex. There is evidence from monkey as well as human neuroimaging studies (e.g. Nobre et al. (1997), Corbetta (1998)) that an interconnected network of cortical areas exert control over modality-specific populations of extrastriate neurons and modulate their responses to incoming sensory information. These areas include the posterior parietal cortex, portions of prefrontal cortex, the pulvinar nucleus of the thalamus, the striatum and the superior colliculi.

4.4. Converging evidence from ERPs

The present ERP results indicate that the earliest facilitation of attended inputs occurs at a level beyond the striate cortex starting at 70–75 ms post-stimulus (the onset of the P1 attention effect). The calculated source of this early facilitation was near the dorsal occipital foci of fMRI activation (both attention-related and sensory-related) in the vicinity of area V3 and in more anterior regions of the middle occipital gyrus. Similar dorsal sources for the P1 attention effect have been reported in previous studies that presented stimuli to the lower (Woldorff et al., 1997) but not upper (Heinze et al., 1994a; Mangun et al., 1997) visual fields, suggesting that this early facilitation occurs in retinotopically organized extrastriate areas. In contrast, the source of the later phase of the P1 effect (104–136 ms) was situated in ventral occipital cortex in the region of area V4v and posterior fusiform gyrus; this activity may be attributed to enhanced processing of the visual target information in ventral stream areas specialized for pattern and object recognition (Heinze et al., 1994a; Mangun & Hillyard, 1995; Clark & Hillyard, 1996; Mangun et al., 1997; Hillyard & Anllo-Vento, 1998). The dipole pair accounting for the anterior N1 attention effect could not be related to the fMRI data since the location of these dipoles was in superior parietal cortex beyond (anterior to) the imaged brain volume.

As in previous studies, the earlier C1 component did not vary in amplitude or latency as a function of attention. Although the neural generators of surface recorded ERPs cannot be localized with the same degree of certainty as can hemodynamic changes using fMRI, the localization of the C1 dipole to the calcarine fissure, as well as its short onset latency (50 ms) and its retinotopic properties (Clark et al., 1995; Mangun, 1995) are strongly indicative of a source in area V1. In the present study, the calculated location of the C1 dipole also lay within the calcarine fissure and was in close proximity to the clusters of fMRI activation in area V1 produced both during passive stimulation and spatial attention. It remains then to be explained why it is that the C1 component having its putative origin in striate cortex is unaffected by attention while fMRI indicates the presence of robust attentional modulations in the very same striate areas.

4.5. Nature of attention-related striate activity

If the modulation of activity in V1 seen with fMRI does not represent a change in the initial geniculo-striate input, reflected in the C1 component, what then is the role of the striate cortex in spatial attention? One hypothesis that draws support from both animal (Roelfsema et al., 1998; Vidyasagar, 1998; Mehta et al., 2000a) and human (Aine, Supek, & George, 1995; Gratton, 1997) studies is that attentional modulation of striate activity occurs with a longer latency than the initial evoked response in striate cortex. These delayed modulations are proposed to represent reentrant feedback of enhanced visual signals into V1 from higher extrastriate or parietal areas. Recent single-unit recordings (Roelfsema et al., 1998; Vidyasagar, 1998) have reported modulations of V1 neuronal activity starting as late as 200 ms post-stimulus, well beyond the peak of the initial sensory-evoked response which, in both of these studies, was found to remain unchanged as a function of the animal's attentional state.

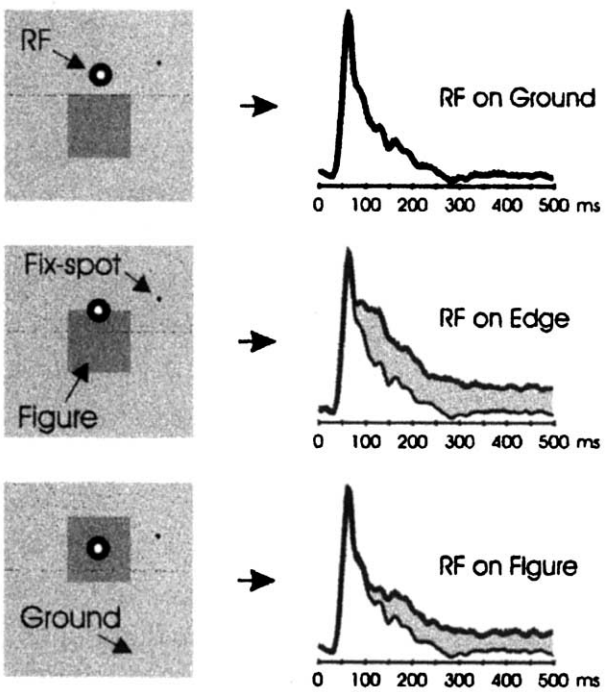

Fig. 9. Contextual modulation of V1 cells in the monkey. The gray shading indicates an enhancement of V1 responses when the cell's receptive field (RF) is on the figure or on the boundary between figure and ground relative to when it falls on the background. Note the delayed nature of this contextual effect and also that in all three cases the initial sensory-evoked response of the cell is identical. From Lamme & Spekreijse (2000).

The new dipole model presented here (Figs. 7 and 8) provides evidence in accord with the hypothesis of a delayed attention effect in area V1. The neural source represented by the calcarine dipole that was fit to the early, attention-insensitive C1 component showed a long-latency modulation with attention in the 160–260 ms range. This analysis is consistent with the proposition that both the C1 and the delayed attention effect originate from co-localized neural generators in the primary visual cortex. A similar conclusion was reached by Aine et al. (1995), who reported long-latency (130–160 ms) modulation of the event-related magnetic field response localized to the calcarine fissure during spatial attention. It should be cautioned, however, that in the absence of direct intracranial recordings from the different cortical areas, it is difficult to rule out possible contributions from similarly oriented neural generators in adjacent extrastriate cortical areas.

The waveform of the delayed attention effect reported here closely resembles that observed for single-cell recordings from V1 in monkeys when modulated by the contextual influence of stimulus contours outside the classical receptive field (RF). These modulatory effects of surrounding contours began at 80–100 ms post-stimulus onset, while the initial afferent response of the cell was unaffected (Fig. 9). The similarity of these long-latency modulations in monkeys and humans suggests that spatial attention may affect the firing of V1 cells in the same delayed manner as do contextual stimulus factors, perhaps using the same neural feedback circuitry (Ito & Gilbert, 1999; Lamme & Spekreijse, 2000).

Modulatory reentrant signals into V1 may be a useful mechanism for stimulus selection in cases where multiple competing stimuli are simultaneously present within the RFs of extrastriate cells. In order to selectively facilitate the processing of relevant objects surrounded by confusable distractors, information fed back into area V1 from higher areas may specifically enhance responses within a subset of V1 cells that code the attended region of space. Neurons in V1 have very small receptive fields and thus have a high degree of retinotopic specificity; maintaining this locational selectivity may be essential for distinguishing among objects appearing in close proximity of one another. Whatever the exact mechanism, the long-latency attention effects observed here and in previous studies (Aine et al., 1995; Gratton, 1997) provide no support for the hypothesis that spatial attention modulates the initial passage of visual input from the lateral geniculate nucleus through area V1 (Skinner & Yingling, 1977; Crick, 1984) even under these cluttered field conditions.

An alternative hypothesis that might account for the mismatch between the hemodynamic and electrophysiological effects in striate cortex obtained in the present study is that the V1 activity observed with fMRI is produced by a top-down 'bias signal' that engenders sustained, attention-related increases in neural discharge rates without necessarily modulating the stimulus-evoked response. This type of attentional bias effect has been observed in extrastriate neurons in monkeys by Desimone and colleagues (Desimone & Duncan, 1995; Luck et al., 1997). These authors have shown that some cells in area V2 and V4 show elevated baseline firing rates while the animal's attention is engaged at locations inside the cell's receptive field. This activity was seen prior to the sensory response elicited by the attended stimulus, which itself was not modulated by attention, as well as during periods without any sensory response such as when the stimulus was presented at unattended locations falling outside the neuron's receptive field. Sustained fMRI activations in extrastriate visual areas have been observed during periods of stimulus anticipation (Kastner et al., 1999; Hopfinger et al., 2000); these effects may be related to the baseline firing changes seen in animal studies.

The delayed-feedback and tonic-bias hypotheses described above are not mutually exclusive nor are they the only two alternatives for explaining the absence of attentional modulation on the evoked C1 component. Another possibility might be that focal attention produces high frequency oscillations in the activity of V1

cells that are not time-locked to the eliciting stimulus (Brosch, Bauer, & Eckhorn, 1997; Engel, Roelfsema, Fries, Brecht, & Singer, 1997a) (i.e. they occur at varying latencies) and thus would not be detected in averaged ERPs. Similarly, attention effects in V1 might escape detection in ERP recordings if the anatomical configuration of the active striate neurons did not produce a dipolar voltage field or if it were so weak as to be masked by the stronger sources that were concurrently active in extrastriate cortex. Further work is needed to distinguish among these alternative mechanisms.

5. Conclusions

The findings presented here, in conjunction with those of previous studies, help to reveal the timing and neuroanatomical bases of stimulus selection processes and to characterize the respective roles of extrastriate and striate cortex in visuospatial attention. In particular, these data suggest that spatially-focused attention brings about selective changes in the processing of relevant-location information starting at approximately 70 ms post-stimulus onset (the onset of the P1) and that these changes are correlated with enhanced blood-flow in both dorsal and ventral extrastriate cortex. The earliest ERP spatial attention effects (the late and early phases of the P1 component) were co-localized with enhanced blood-flow in both dorsal and ventral extrastriate cortex, in or near areas V3 and V4, respectively. A comparison between conditions of passive visual stimulation and the focused attention task showed that attention modulates the activity of many of the same extrastriate areas involved in sensory processing. This finding is consistent with a sensory gain hypothesis whereby spatial attention acts to increase the signal-to-noise ratio of neurons involved in processing the physical characteristics of visual stimuli rather than to recruit a different population of active neurons.

Functional neuroimaging also revealed robust attentional modulations in area V1. However, ERP recordings suggested that this attention-related striate activity did not represent a modulation of the initial sensory evoked response elicited by attended stimuli (indexed electrophysiologically by the short-latency C1 component). Several possible explanations were offered to account for this apparent discrepancy between the ERP and fMRI results, but a new dipole source analysis was consistent with the hypothesis that the increased neural activity in V1 revealed by fMRI reflects delayed reentrant signals from higher extrastriate cortical areas. Further research along these lines is needed to conclusively define the precise role of striate cortex in spatial attention, but the data presented here illustrate how converging evidence from neuroimaging and electrophysiological techniques may be used to reveal both spatial and temporal properties of neural activity during selective attention.

Acknowledgements

We thank Matt Marlow and Cecelia Kemper for technical assistance. Supported by grants from NIMH (MH25594) and NIH (NS36722).

References

Aine, C. J., Supek, S., & George, J. S. (1995). Temporal dynamics of visual-evoked neuromagnetic sources: effects of stimulus parameters and selective attention. *International Journal of Neuroscience*, *80*, 79–104.

Anllo-Vento, L., Luck, S. J., & Hillyard, S. A. (1998). Spatio-temporal dynamics of attention to color: evidence from human electrophysiology. *Human Brain Mapping*, *6*, 216–238.

Brefczynski, J. A., & DeYoe, E. A. (1999). A physiological correlate of the 'spotlight' of visual attention. *Nature Neuroscience*, *2*, 370–374.

Brosch, M., Bauer, R., & Eckhorn, R. (1997). Stimulus-dependent modulation of correlated high-frequency oscillations in cat visual cortex. *Cerebral Cortex*, *7*, 70–76.

Buchel, C., Josephs, O., Rees, G., Turner, R., Frith, C. D., & Friston, K. J. (1998). The functional anatomy of attention to visual motion: a functional MRI study. *Brain*, *121*, 1281–1294.

Chawla, D., Rees, G., & Friston, K. J. (1999). The physiological basis of attentional modulation in extrastriate visual areas. *Nature Neuroscience*, *2*, 671–676.

Clark, V. P., & Hillyard, S. A. (1996). Spatial selective attention affects early extrastriate but not striate components of the visual evoked potential. *Journal of Cognitive Neuroscience*, *8*, 387–402.

Clark, V. P., Fan, S., & Hillyard, S. A. (1995). Identification of early visually evoked potential generators by retinotopic and topographic analyses. *Human Brain Mapping*, *2*, 170–187.

Colby, C. L. (1991). The neuroanatomy and neurophysiology of attention. *Journal of Child Neurology*, *6*, 90–118.

Corbetta, M. (1998). Frontoparietal cortical networks for directing attention and the eye to visual locations: identical, independent, or overlapping neural systems? *Proceedings of the National Academy of Sciences*, *95*, 831–838.

Corbetta, M., Kincade, J. M., Ollinger, J. M., McAvoy, M. P., & Shulman, G. L. (2000). Voluntary orienting is dissociated from target detection in human posterior parietal cortex. *Nature Neuroscience*, *3*, 292–297.

Cox, R. W. (1996). AFNI -Software for analysis and visualization of functional magnetic resonance neuroimages. *Computers and Biomedical Research*, *29*, 162–173.

Crick, F. (1984). Function of the thalamic reticular complex: the searchlight hypothesis. *Proceedings of the National Academy of Sciences*, *81*, 4586–4590.

Desimone, R. (1998). Visual attention mediated by biased competition in extrastriate visual cortex. *Philosophical Transactions of the Royal Society*, *353*, 1245–1255.

Desimone, R., & Duncan, J. (1995). Neural mechanisms of selective visual attention. *Annual Review of Neuroscience*, *18*, 193–222.

DeYoe, E. A., Carman, G. J., Bandettini, P., et al. (1996). Mapping striate and extrastriate visual areas in human cerebral cortex. *Proceedings of the National Academy of Sciences*, *93*, 2382–2386.

Engel, A. K., Roelfsema, P. R., Fries, P., Brecht, M., & Singer, W. (1997a). Role of the temporal domain for response selection and perceptual binding. *Cerebral Cortex*, *7*, 571–582.

Engel, S. A., Glover, G. H., & Wandell, B. A. (1997b). Retinotopic organization in human visual cortex and the spatial precision of functional MRI. *Cerebral Cortex*, *7*, 181–192.

Gandhi, S. P., Heeger, D. J., & Boynton, G. M. (1999). Spatial attention affects brain activity in human primary visual cortex. *Proceedings of the National Academy of Sciences*, *96*, 3314–3319.

Gomez, C. M., Clark, V. P., Luck, S. J., Fan, S., & Hillyard, S. A. (1994). Sources of attention-sensitive visual event-related potentials. *Brain Topography*, *7*, 41–51.

Gratton, G. (1997). Attention and probability effects in the human occipital cortex: an optical imaging study. *NeuroReport*, *8*, 1749–1753.

Hawkins, H. L., Hillyard, S. A., Luck, S. J., Mouloua, M., Downing, C. J., & Woodward, D. P. (1990). Visual attention modulates signal detectability. *Journal of Experimental Psychology: Human Perception and Performance*, *16*, 802–811.

Heinze, H. J., Luck, S. J., Muente, T. F., Goes, A., Mangun, G. R., & Hillyard, S. A. (1994a). Attention to adjacent and separate positions in space: an electrophysiological analysis. *Perception and Psychophysics*, *56*, 42–52.

Heinze, H. J., Mangun, G. R., Burchert, W., et al. (1994b). Combined spatial and temporal imaging of brain activity during visual selective attention in humans. *Nature*, *372*, 543–546.

Hillyard, S. A., & Anllo-Vento, L. (1998). Event-related brain potentials in the study of visual selective attention. *Proceedings of the National Academy of Sciences*, *95*, 781–787.

Hillyard, S. A., Vogel, E. K., & Luck, S. J. (1998). Sensory gain control (amplification) as a mechanism of selective attention: electrophysiological and neuroimaging evidence. *Philosophical Transactions of the Royal Society Series B*, *353*, 1257–1270.

Hopfinger, J. B., Buonocore, M. H., & Mangun, G. R. (2000). The neural mechanisms of top-down attentional control. *Nature Neuroscience*, *3*, 284–291.

Hupe, J. M., James, A. C., Payne, B. R., Lomber, S. G., Girard, P., & Bullier, J. (1998). Cortical feedback improves discrimination between figure and background by V1, V2 and V3 neurons. *Nature*, *394*, 784–787.

Ito, M., & Gilbert, C. D. (1999). Attention modulates contextual influences in the primary visual cortex of alert monkeys. *Neuron*, *22*, 593–604.

Jancke, L., Mirzazade, S., & Shah, N. J. (1999). Attention modulates the blood oxygen level dependent response in the primary visual cortex measured with functional magnetic resonance imaging. *Naturwissenschaften*, *86*, 79–81.

Kastner, S., DeWeerd, P., Desimone, R., & Ungerleider, L. (1998). Mechanisms of directed attention in the human extrastriate cortex as revealed by functional MRI. *Science*, *282*, 108–111.

Kastner, S., Pinsk, M. A., DeWeerd, P., Desimone, R., & Ungerleider, L. G. (1999). Increased activity in human visual cortex during directed attention in the absence of visual stimulation. *Neuron*, *22*, 751–761.

LaBerge, D. (1995). *Attention processing: the brain's act of mindfulness*. Cambridge, MA: Harvard University Press.

Lamme, V. A. F., & Spekreijse, H. (2000). Contextual modulation in primary visual cortex and scene perception. In M. S. Gazzaniga, *The new cognitive neurosciences* (pp. 279–290). Cambridge, MA: MIT Press.

Lange, J. J., Wijers, A. A., Mulder, L. J. M., & Mulder, G. (1998). Color selection and location selection in ERPs: differences, similarities and 'neural specificity'. *Biological Psychology*, *48*, 153–182.

Luck, S. J., Hillyard, S. A., Mouloua, M., Woldorff, M. G., Clark, V. P., & Hawkins, H. L. (1994). Effects of spatial cueing on luminance detectability: psychophysical and electrophysiological evidence for early selection. *Journal of Experimental Psychology: Human Perception and Performance*, *20*, 887–904.

Luck, S. J., Chelazzi, L., Hillyard, S. A., & Desimone, R. (1997). Neural mechanisms of spatial selective attention to areas V1, V2, and V4 of Macaque visual cortex. *Journal of Neurophysiology*, *77*, 24–42.

Mangun, G. R. (1995). Neural mechanisms of visual selective attention. *Psychophysiology*, *32*, 4–18.

Mangun, G. R., & Hillyard, S. A. (1995). Attention: mechanisms and models. In M. D. Rugg, & M. G. H. Coles, *Electrophysiology of mind — event-related potentials and cognition* (pp. 40–85). London: Oxford University Press.

Mangun, G. R., Hopfinger, J., Kussmaul, C. L., Fletcher, E., & Heinze, H. J. (1997). Covariations in ERP and PET measures of spatial selective attention in human extrastriate visual cortex. *Human Brain Mapping*, *5*, 273–279.

Martinez, A. 1999. Cortical mechanisms of selective attention to spatial and non-spatial stimulus features. Doctoral Dissertation in Psychology, University of California, San Diego.

Martinez, A., Anllo-Vento, L., Sereno, M. I., et al. (1999). Involvement of striate and extrastriate visual cortical areas in spatial attention. *Nature Neuroscience*, *2*, 364–369.

Maunsell, J. H. R., & McAdams, C. J. (2000). Effects of attention on neuronal response properties in visual cerebral cortex. In M. Gazzaniga, *The new cognitive neurosciences*. Cambridge, MA: MIT Press.

McAdams, C. J., & Maunsell, J. C. (1999). Effects of attention on orientation-tuning functions of single neurons in macaque cortical area V4. *Journal of Neuroscience*, *19*, 431–441.

Mehta, A. D., Ulbert, I., & Schroeder, C. E. (2000a). Intermodal selective attention in monkeys II: physiological mechanisms of modulation. *Cerebral Cortex*, *10*, 359–370.

Mehta, A. D., Ulbert, I., & Schroeder, C. E. (2000b). Intermodal selective attention in monkeys I: distribution and timing of effects across visual areas. *Cerebral Cortex*, *10*, 343–358.

Mesulam, M. M. (1990). Large-scale neurocognitive networks and distributed processing for attention, language and memory. *Annals of Neurology*, *28*, 597–613.

Motter, B. C. (1993). Focal attention produces spatially selective processing in visual cortical areas V1, V2 and V4 in the presence of competing stimuli. *Journal of Neurophysiology*, *70*, 909–919.

Nobre, A. C., Sebestyen, G. N., Gitelman, D. R., Mesulam, M. M., Frackowiak, R. S. J., & Frith, C. D. (1997). Functional localization of the system for visuospatial attention using positron-emission tomography. *Brain*, *120*, 515–533.

Posner, M. I., & Dehaene, S. (1994). Attentional networks. *Trends in Neurosciences*, *17*, 75–79.

Posner, M. I., & Gilbert, C. D. (1999). Attention and primary visual cortex. *Proceedings of the National Academy of Science*, *96*, 2585–2587.

Reynolds, J. H., Chelazzi, L., & Desimone, R. (1999). Competitive mechanisms subserve attention in macaque areas v2 and v4. *Journal of Neuroscience*, *19*, 1736–1753.

Roelfsema, P. R., Lamme, V. A. F., & Spekreijse, H. (1998). Object-based attention in the primary visual cortex of the macaque monkey. *Nature*, *395*, 376–381.

Scherg, M. (1990). Fundamentals of dipole source potential analysis. In F. Grandori, M. Hoke, & G. L. Romani, *Auditory evoked magnetic fields and potentials. advanced audiology*, vol. 6 (pp. 40–69). Basel: Karger.

Sengpiel, F., & Huebener, M. (1999). Visual attention: spotlight on the primary visual cortex. *Current Biology*, *9*, 318–321.

Sereno, M. I., Dale, A. M., Reppas, J. B., et al. (1995). Borders of multiple visual areas in humans revealed by functional magnetic resonance imaging. *Science*, *268*, 889–893.

Shulman, G. L., Corbetta, M., Buckner, R. L., et al. (1997). Top-down modulation of early sensory cortex. *Cerebral Cortex*, *7*, 193–206.

Skinner, J. E., Yingling, C. D. (1977). Central gating mechanisms that regulate event-related potentials and behavior. In: Desmedt, J. E. (Ed.), *Attention, voluntary contraction and event-related cerebral potentials. Progress in clinical neurophysiology*, Vol. 1, pp. 30–69.

Smith, A. T., Singh, K. D., & Greenlee, M. W. (2000). Attentional suppression of activity in the human visual cortex. *NeuroReport*, *11*, 271–277.

Somers, D. C., Dale, A. M., Seiffert, A. E., & Totell, R. B. H. (1999). Functional MRI reveals spatially specific attentional modulation in human primary visual cortex. *Proceedings of the National Academy of Sciences*, *96*, 1663–1668.

Talairach, J., & Tournoux, P. (1988). *Co-planar stereotaxic atlas of the human brain: 3-dimensional proportional system: an approach to cerebral imaging*. New York: Thieme.

Theeuwes, J., Kramer, A. F., & Atchley, P. (1999). Attentional effects on preattentive vision: spatial precues affect the detection of simple features. *Journal of Experimental Psychology*, *25*, 341–347.

Tootell, R. B. H., Reppas, J. B., Kwong, K. K., et al. (1995). Functional analysis of human MT and related visual cortical areas using magnetic resonance imaging. *Journal of Neuroscience*, *15*, 3215–3230.

Tootell, R. B., Mendola, J. D., & Hadjikhani, N. K. (1997). Functional analysis of V3A and related areas in human visual cortex. *Journal of Neuroscience*, *17*, 7060–7078.

Tootell, R. B. H., Hadjikhani, N., Hall, E. K., et al. (1998). The retinotopy of visual spatial attention. *Neuron*, *21*, 1409–1422.

Treue, S., & Maunsell, J. H. R. (1996). Attentional modulation of visual motion processing in cortical areas MT and MST. *Nature*, *382*, 539–541.

Vidyasagar, T. R. (1998). Gating of neuronal responses in macaque primary visual cortex by an attentional spotlight. *NeuroReport*, *9*, 1947–1952.

Vidyasagar, T. R. (1999). A neuronal model of attentional spotlight: parietal guiding the temporal. *Brain Research Reviews*, *30*, 66–76.

Watanabe, T., Harner, A. M., Miyauchi, S., et al. (1998a). Task-dependent influences of attention on the activation of human primary visual cortex. *Proceedings of the National Academy of Sciences*, *95*, 11489–11492.

Watanabe, T., Sasaki, Y., Miyauchi, S., et al. (1998b). Attention-regulated activity in human primary visual cortex. *Journal of Neurophysiology*, *79*, 2218–2221.

Wijers, A. A., Lange, J. J., Mulder, G., & Mulder, L. J. M. (1997). An ERP study of visual spatial attention and letter target detection for isoluminant and nonisoluminant stimuli. *Psychophysiology*, *34*, 553–565.

Woldorff, M. (1993). Distortion of ERP averages due to overlap from temporally adjacent ERPS: analysis and correction. *Psychophysiology*, *30*, 98–119.

Woldorff, M. G., Fox, P. T., Matzke, M., et al. (1997). Retinotopic organization of the early visual-spatial attention effects as revealed by PET and ERPs. *Human Brain Mapping*, *5*, 280–286.

Worden, M., & Schneider, W. (1996). Visuospatial attentional selection examined with functional magnetic resonance imaging. *Society for Neuroscience Abstracts*, *22*, 1856.

Wright, R. D. (1998). *Visual attention*, vol. 8. London: Oxford University Press.